JOURNAL OF Materials CHEMISTRY

ZrO_2 bubbles from core–shell nanoparticles†

A. Sreekumaran Nair, Renjis T. Tom, V. Suryanarayanan and T. Pradeep*

Department of Chemistry and Regional Sophisticated Instrumentation Centre, Indian Institute of Technology Madras, Chennai 600 036, India. E-mail: pradeep@iitm.ac.in; Fax: +91-44-2257 0509 or 0545

Received 31st October 2002, Accepted 6th December 2002
First published as an Advance Article on the web 7th January 2003

Selective removal of metal cores from core–shell Ag@ZrO_2 (ZrO_2 coated Ag) and Au@ZrO_2 (ZrO_2 coated Au) nanoparticles result in stable and freely suspendable oxide nanobubbles of varying dimensions, both in thickness and in diameter. The metal core is removed by a newly found reaction in which halocarbons, generally chlorides, oxidise the metal core and leach out the metal ions. Reduction in the surface plasmon excitation intensity and decrease in the voltammetric current during metal core removal were used to study the process.

Introduction

The science and technology of nanostructured materials is advancing at a rapid pace. Most of the present day activity in this area is on nanoparticles, especially semiconductor and metal quantum dots.[1] We have been particularly interested in monolayer protected metal clusters.[2] Electronic, magnetic and catalytic properties of the nanostructured materials depend mainly on their size and shape.[3] They are also useful in optical data storage and solar energy conversion.[4,5] Metal nanoparticles have peculiar and intense colour originating from the coherent electron motion which gives rise to the surface plasmon absorption.[6] Resonance frequency and the width of the plasmon absorption band depend on the nanoparticle size.[7] Core–shell nanomaterials are the recent addendum to nanoscience.[8–20] The surfaces of these particles, being reactive, need to be protected with appropriate covers and monolayer protection is often used. Different metal oxides of desired thickness are coated on the particle with appropriate chemistry. Several approaches have been used recently to make silica,[9] titania[10] and zirconia[11] covered noble metal clusters. The synthesis and characterization of TiO_2 covered Ag nanoparticles has been reported by Liz-Marzan *et al.*[10] and we have extended this method to ZrO_2 covered Ag and Au nanoparticles.[12] The coating of metal nanoparticles with a thin layer of oxide material makes it possible to control inter-particle and particle–matrix interactions thereby improving their potential for applications.[10] The core–shell geometry causes enhancement in the luminescence of semiconductor nanoparticles,[13] chemical and colloidal stability,[14] charging of metal cores[15] and optimization of magnetic properties.[16] In this paper we show that the nanocore can be leached completely by a new kind of chemistry and the shell can be preserved intact leading to oxide nanobubbles of varying thicknesses. These bubbles form freestanding solutions in organic media and bulk materials with interesting properties which can be obtained with appropriate scale-up. It may be noted that leaching of metal cores has been demonstrated for Ag@TiO_2[17] and Au@SiO_2[18] already; these used reactions with OH^- and CN^-, respectively.

†Electronic Supplementary Information (ESI) available: Time dependent UV-visible spectra of the reaction between Au@ZrO_2 and CCl_4. See http://www.rsc.org/suppdata/jm/b2/b210734a/

Experimental

$AgNO_3$ was purchased from Qualigens chemicals, India and zirconium(IV) propoxide was from Aldrich. All the other chemicals used in the experiments were from local sources and the solvents were distilled prior to use. Water was of nanopure quality. Zirconia covered silver nanoparticles were prepared by a one-pot synthesis. A similar procedure has been reported for titania coated silver particles.[14] 30 mg of $AgNO_3$ were dissolved in a mixture of 15 ml dimethylformamide (DMF) and 5 ml H_2O. Another solution containing 200 μl of acetyl acetone and 250 μl of zirconium(IV) propoxide in 40 ml of 2-propanol was prepared. The two solutions were mixed and refluxed for 45 min at 90 °C till a greenish-black colour appeared. This solution consists of core–shell particles of ~30–60 nm core diameter and ~3 nm shell thickness.[12] For getting nanobubbles, 4 ml of the as prepared cluster solution was mixed with 1 ml each of CCl_4 or benzyl chloride separately. The reaction happened over a period of several hours (see below) and the solution turned colourless. Silver ions were leached out and precipitated as AgCl during the reaction. This halocarbon chemistry on metal nanoparticles will be published separately.[21] Bubbles were precipitated from solution by decreasing the polarity of the medium and by adding solvents such as toluene. The nearly dry precipitate was re-dispersed in 2-propanol and the process was repeated for purification; the dry powders were difficult to re-disperse.

Transmission electron microscopy (TEM) measurements were performed with a Philips CM12 microscope working at 120 KeV acceleration. The sample solution was drop-casted on carbon coated copper grids. Scanning electron micrographs of solution-coated films were taken with a JEOL 30 KV machine. X-ray diffraction studies were carried out with a Shimadzu XD-D1 diffractometer with Cu Kα radiation (30 kV, 20 mA). The samples were spread on antireflecting glass slides and were wetted with acetone to obtain a uniform film. Acetone was blown dry and the slide was mounted on the diffractometer. IR spectroscopic measurements were performed with a Perkin Elmer Spectrum One FT-IR spectrometer. All samples were prepared in the form of 1% (by weight) KBr pellets. UV-visible spectra were measured in a Perkin Elmer Lambda 25 UV/VIS spectrophotometer. Cyclic voltammograms were obtained on an Electrochemical Analyzer (CH Instruments Model 600A) in a standard three-electrode cell comprising Pt disk (area = 0.8 mm^2) working electrode, platinum foil counter electrode

DOI: 10.1039/b210734a

and Ag/AgCl reference electrode. A 0.1 M tetrabutylammonium hexafluorophosphate (TBAHFP) solution in CH_3CN was taken as the solvent-supporting electrolyte system for the cyclic voltammetry experiments. For recording cyclic voltammograms, 4 ml of the nanoparticle solution was dissolved in 10 ml of the supporting electrolyte medium. For the bubble reaction, 1 ml of the reactant was added and voltammograms were measured.

Results and discussion

The UV-visible absorption spectrum of $Ag@ZrO_2$ shows the characteristic surface plasmon resonance feature at 425 nm. The shift in the plasmon resonance of Ag from the characteristic value of 400 nm is due to the dielectric cover surrounding the cluster.[14] Depending on the thickness of the oxide cover, the plasmon frequency can be shifted, thereby changing the colour.[19] Both of these spectral features (width and position) are related to the high dielectric constant of ZrO_2[22] in contact with the Ag surface. Mie first described this phenomenon theoretically by solving Maxwell's equation for a radiation field interacting with a spherical metal particle under the appropriate boundary conditions.[23] The only material related functions in the expression are the complex dielectric function of the metal and dielectric constant of the surrounding medium. The surrounding medium, also referred to as the capping material (oxide matrix), is of great importance as it prevents aggregation.[14]

In Fig. 1A we show the UV-visible spectra of the $Ag@ZrO_2$ solution as a function of reaction time with CCl_4. The traces were recorded at an interval of 30 min after the addition of CCl_4. The intensity of the plasmon absorption band decreases with the passage of time, which implies the selective leaching of the Ag core. Finally the plasmon absorption is lost completely indicating the completion of selective leaching of the core or the formation of freely suspendable ZrO_2 nanobubbles. The grey-white precipitate formed was analyzed with XRD, which gave the characteristic peaks of AgCl. The bubbles can be precipitated from the colourless solution by adding toluene and can be redissolved back into 2-propanol as mentioned above.

Fig. 1B represents the UV-visible spectra for the time dependent reaction between $Ag@ZrO_2$ and benzyl chloride. The traces were recorded at an interval of 10 min. Note that benzyl chloride is more reactive than CCl_4 and the reduction in plasmon is abrupt. While the CCl_4 reaction takes 7 h and 30 min for the complete disappearence of plasmon, benzyl chloride takes only 1 h 50 min to do so. The gradual decrease in the intensity of plasmon absorption implies the selective removal of core from $Ag@ZrO_2$. In both the cases, it is important to note that the plasmon does not show any shift as the reaction proceeds. This suggests that the halocarbon reacts directly at the surface and no long-lived adsorbed state is involved.

Fig. 2 shows the transmission electron micrograph of the particles after the removal of the metal core. A close-up view of a nanoparticle with the shell is shown in the inset. It can be seen that the shell is of a thickness of $\sim$3 nm and it covers the core completely. The typical core size is 50 nm. Although the particle shown here is spherical, other geometries were also seen. A micrograph of the materials after core removal shows nanobubbles and the cores are completely absent. The picture shows several morphologies of the bubbles, representing the size distribution of the parent particles. Coalescence of smaller bubbles to give larger bubbles is also evident from the TEM image (indicated by a broken arrow). The shells do not show any diffraction while the cores show a characteristic diffraction pattern with a [111] zone axis.

As noted by Liz-Marzan and colleagues,[20] the synthesis also leads to smaller size particles. These are in the size range of 10 nm and the cores are lost for these particles as well upon reaction. The shells are visible and the spherical morphology is distinct (Fig. 3). Larger bubbles could be imaged by SEM. The SEM image in Fig. 4 clearly shows the spherical morphology of a large isolated ZrO_2 bubble.

The destruction of nanocores was evident in cyclic voltammetric studies also. For this study, 1 ml of benzyl chloride was added to the reaction mixture containing 4 ml of the colloidal solution and 10 ml of solvent-supporting electrolyte system. Typical superimposed time dependent votammograms obtained by the treatment of $Ag@ZrO_2$ nanocomposities with CCl_4 taken at 30 min intervals of time (at a sweep rate of 300 mV s^{-1}) are shown in Fig. 5A. Curve (a) shows the cyclic voltammogram of $Ag@ZrO_2$ in the absence of CCl_4 and (b) to (g) in the presence of CCl_4, recorded at 30 min intervals.

$Ag@ZrO_2$ shows characteristic reversible redox couple

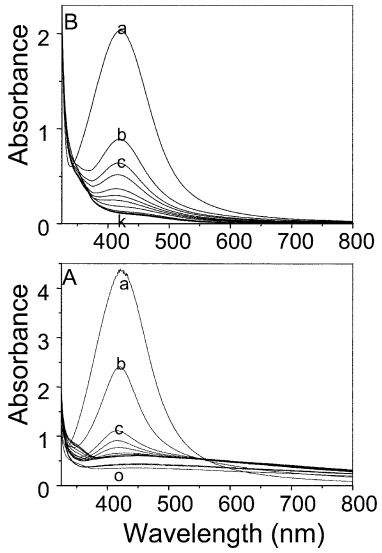

Fig. 1 Time dependent UV–visible spectra of the reaction of $Ag@ZrO_2$ with (A) CCl_4 and (B) benzyl chloride indicating the selective leaching of the metal core. Traces *a* correspond to the parent material. In (A) the traces were recorded after every 30 min and in (B) after every 10 min (after addition of CCl_4 and benzyl chloride, respectively).

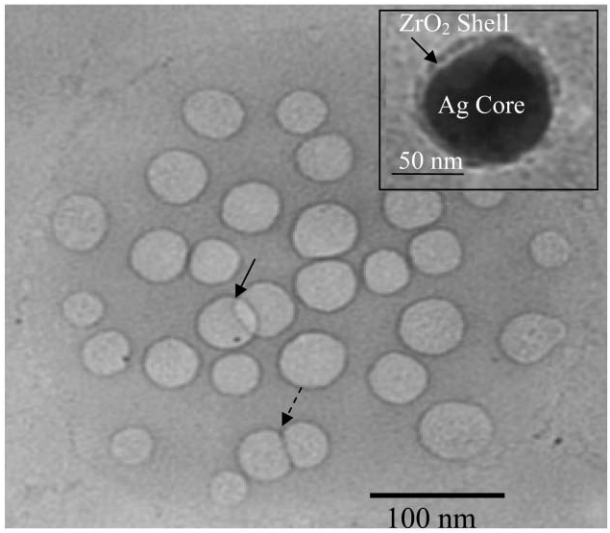

Fig. 2 TEM micrograph of the nanobubbles formed from $Ag@ZrO_2$ by reaction with CCl_4. An expanded micrograph of a core shell particle is shown in the inset. The shell is of 3 nm thickness. The core and shell are marked. Note that in the nanobubble, two particles are imaged one over the other (arrow). There appears a fusion of two particles, shown by a broken arrow.

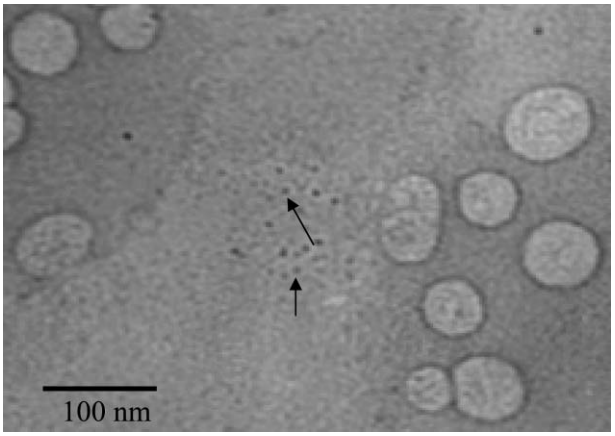

Fig. 3 TEM image of smaller and larger nanobubbles. Some of the smaller particles may contain metal particles, but most of them are hollow as shown by arrows. There was no electron diffraction from these areas.

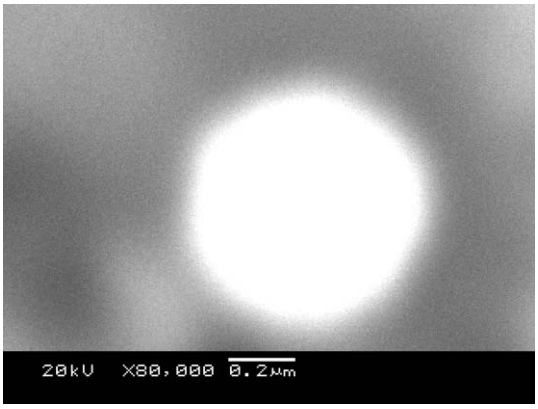

Fig. 4 Scanning electron microscopic image of an isolated ZrO_2 bubble.

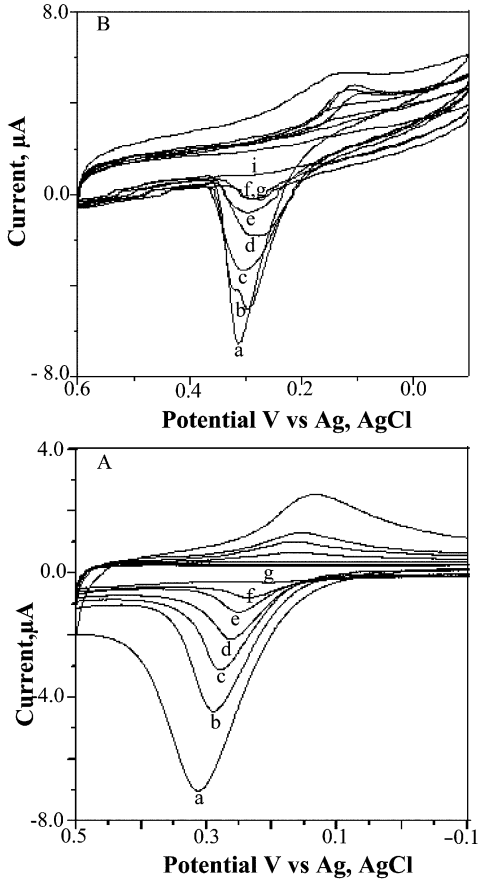

Fig. 5 Time dependent cyclic voltammograms obtained by the reaction between $Ag@ZrO_2$ and (A) 1 ml carbon tetrachloride and (B) 1 ml benzyl chloride on a Pt electrode. The medium is CH_3CN containing 0.1 M tetrabutylammonium hexafluorophosphate (TBAHFP). Curve (a) shows the voltammogram in the absence of reactant and successive curves in its presence.

centered at $E_{1/2} = 0.215$ V with a peak separation of ΔE_p 0.190 V. The sharp and symmetrical anodic peak at 0.310 V has FWHM of 60 mV suggesting one electron transfer of silver nanoclusters[24,25] ($Ag_n \rightarrow Ag_n^+ + e$) (curve (a)). The peak potential and current vary linearly with scan rate. The surface coverage calculated from the area under the cathodic peak is found to be larger than the anodic peak. This has also been observed earlier, in the case of studies related to dodecanethiol capped silver clusters on Pt electrodes dispersed in 0.1 M TBAHFP/toluene and acetonitrile medium.[25]

With the addition of CCl_4, it is observed that both the characteristic anodic and cathodic peak current intensities decrease (curves (b) to (f)) and finally the curve becomes flat, giving the original background current of the Pt electrode (curve (g)). There is also some shift in the anodic peak potential towards a negative value during the successive scans in which the value of ΔE_p decreases. This may be due to the decrease in E_{pa} values or change in the oxidation potentials of the redox system. Decrease in the redox current is due to the removal of electroactive Ag nanoparticles from the shell by the halogen, which precipitates Ag as AgCl.

A similar type of reaction was noticed with benzyl chloride and $CHBr_3$. Typical superimposed time dependent voltammograms obtained during the reaction of $Ag@ZrO_2$ with benzyl chloride under otherwise identical experimental conditions are shown in Fig. 5B. From the voltammetric curves it is evident that complete leaching of the Ag nanocore occurs. Both the cathodic and anodic peaks appear very sharp in this case unlike the reaction with CCl_4, which are broad (compare the slopes of the voltammetric peaks of Fig. 5A with Fig. 5B). It is also noted that there is a possibility of electro-deposition of silver nanoparticles on the working electrode during this potential cycling and this affected the surface of the Pt electrode during successive measurements.[24] Though we have cleaned the electrode surface by polishing or by chemical treatment, successive recording in case of benzyl chloride gives only a sharp peak. There is a hump in the voltammogram during the first addition of benzyl chloride to the cluster solution (Fig. 5B curve (b)); this may be due to the diffusion of electro-active species near the electrode surface from the earlier run (memory effect). A similar effect was observed for $Ag@TiO_2$ during the formation of TiO_2 nanobubbles. As the benzyl chloride reaction is not as fast as in the case of UV experiments, we conclude that the kinetics of the reaction is influenced by the medium used.

From the data presented it is clear that the nanoshells are porous for ion (and molecular) transport. The voltammetric data support this view. To confirm whether the pores can be blocked by adsorption of functionalized molecules on the oxide surface, we added 2,2′-bipyridyl 4,4′-dicarboxylic acid (a known adsorbate system on oxide nanoparticles[26]) to the solution and the cyclic voltammograms were measured. The peak current decreases as the adsorbate concentration is increased in the solution and it reaches a limiting value. However, addition of benzyl chloride removed the core completely and the peak current reached the background value with increasing exposure time implying that the pores could not be blocked completely.

Increasing the shell thickness (by increasing the oxide precursor concentration in the reaction mixture) lowers the core destruction kinetics. A significant factor influencing the

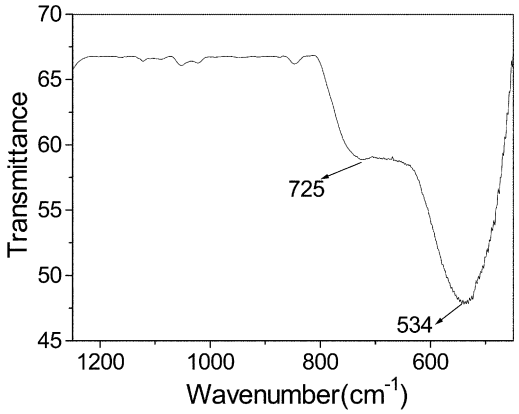

Fig. 6 FT-IR spectrum of the bubbles showing characteristic ZrO_2 features at 534 and 725 cm^{-1}.

kinetics of reaction is the rate of molecular diffusion through the shell. This can be altered by changing the thickness of the shell and by changing the pore dimension or both. It is expected that porosity of the shells will not be significantly different in the two preparations. Thus it may be concluded that the observed effect in core destruction kinetics is due to the change in thickness of the shell. We noticed that large halocarbons such as endosulfan did not go through the pores and the reaction did not occur even after several days. Thus the pore size is a limiting factor in determining the core leaching chemistry.

In order to ascertain the molecular nature of the material, the IR spectrum of the bubble was taken (Fig. 6). The spectrum of ZrO_2 varies depending on the nature of the material, preparative procedures used, solid-state structure, *etc.*[27] However, the features fall always within 300–800 cm^{-1}. The two features found at 534 and 725 cm^{-1} are analogous to the 530 cm^{-1} main feature and 725 cm^{-1} shoulder seen for cubic zirconia.[27] The first feature has been assigned to the triply degenerate F_{1u} mode (transverse mode, TO) and the latter has been assigned to the longitudinal mode (LO). This latter mode can be regarded as the asymmetric Zr–O–Zr stretching. The fact that no additional features are seen in the IR spectrum indicates that the material is essentially a cubic phase; this is expected since as the particle dimension decreases, the packing is expected to be cubic. It supports the nanophase nature of the material. It may also be noted that nanophase cubic zirconia has been made through the monolayer route recently.[28]

The chemistry discussed above works with $Au@ZrO_2$ as well, but with reduced kinetics. As a result of halocarbon exposure, a longer wavelength plasmon emerges with simultaneous reduction in the intensity of the original plasmon at 530 nm, due to changes in the surface dielectric properties. Leaching of the core is evident as the plasmon disappears completely. Time dependent optical absorption spectra during the reaction are given as supplementary information†. Electrochemical features are similar to those of $Ag@ZrO_2$. The nanobubbles can be processed as described in the experimental section.

Conclusion

Free-standing solutions of metal oxide nanobubbles of various diameters have been prepared from $Ag@ZrO_2$ by halocarbon chemistry. The oxide nanobubbles offer many interesting opportunities for catalysis. Compounds with functions such as those with fluorescence, electroactivity, switching properties, *etc.* may be incorporated into the bubbles, giving new materials with interesting properties. The nanobubble formation and their futuristic applications are within the scope of our future work. We are aware that the underlying chemistry of halocarbons at the metal particle surfaces is interesting and more studies are necessary to understand this in detail. Applications of this reaction to halocarbon destruction will be published separately.[21]

Acknowledgements

T. P acknowledges financial support from the Government of India, Ministry of Information Technology and the Space Technology Cell of the Indian Institute of Technology, Madras for his core–shell research programme. Ms. Kanchanamala is thanked for assistance with TEM. One of the authors, V. S thanks CSIR, New Delhi for the award of a Research Associateship.

References

1 A. P. Alivisatos, *J. Phys. Chem.*, 1996, **100**, 13226.
2 N. Sandhyarani and T. Pradeep, *Int. Rev. Phys. Chem.*, in the press.
3 C. A. Foss, G. L. Hornyak, J. A. Stockert and C. R. Martin, *J. Phys. Chem.*, 1994, **98**, 2963.
4 G. Schmid, *Clusters and Colloids: From Theory to Applications*, VCH, Weinheim, 1994.
5 *Electrochemistry in Colloids and Dispersions*, ed. M. Gratzel, R. A. Mackay and J. Texter, VCH, Weinheim, 1994.
6 C. H. Bohren and D. R. Huffman, *Absorbance and Scattering of Light by Small Particles*, John Wiley, New York, 1983.
7 V. Kreibig and M. Vollmer, *Optical Properties of Metal Clusters*, Springer, Berlin, 1995.
8 (*a*) C. J. Kiely, J. G. Fink. Zheng, M. Brust, D. Bethel and D. Schiffrin, *J. Adv. Mater.*, 2000, **12**, 640; (*b*) A. C. Templeton, W. P. Wuelfing and R. W. Murray, *Acc. Chem. Res.*, 2000, **33**, 27; (*c*) L. Yu, Y. Yadong, L. Zhi-Yuan and X. Younan, *Nano Lett.*, 2002, **2**, 785; (*d*) M. M. Y. Chen and A. Katz, *Langmuir*, 2002, **18**, 8566; (*e*) H. Tada, F. Suzuki, S. Ito, T. Akita, K. Tanaka, T. Kawahara and H. Kobayashi, *J. Phys.Chem. B*, 2002, **106**, 8714.
9 (*a*) L. M. Liz-Marzan, M. Giersig and P. Mulvaney, *Langmuir*, 1996, **12**, 4329; (*b*) L. M. Liz-Marzan, M. Giersig and P. Mulvaney, *Chem. Commun.*, 1996, 731; (*c*) L. Tuo, M. Jooho, A. A. Augusto, J. J. Mecholsky, D. R. Talham and J. A. Adair, *Langmuir*, 1999, **15**, 4328.
10 I. P. Santos, D. S. Koktysh, A. A. Mamedov, M. Giersig, N. A. Kotov and L. M. Liz-Marzan, *Langmuir*, 2000, **16**, 2731.
11 V. Eswaranand and T. Pradeep, *J. Mater. Chem.*, 2002, **12**, 2421.
12 R. T. Tom, A. Sreekumaran Nair, M. Aslam, N. Singh, C. L. Nagendra, R. Philip, K. Vijayamohanan and T. Pradeep, *Langmuir*, in the press.
13 X. G. Peng, M. C. Schlamp, A. V. Kadavanich and A. P. Alivisatos, *J. Am. Chem. Soc.*, 1997, **119**, 7019.
14 I. Pastoriza-Santos and L. M. Liz-Marzan, *Langmuir*, 1999, **15**, 948.
15 T. Ung, L. M. Liz-Marzan and P. Mulvaney, *J. Phys. Chem. B*, 1999, **103**, 6770.
16 F. Aliev, M. C-Duarte, A. Mamedov, J. W. Ostrander, M. Giersig, L. M. Liz-Marzan and N. A. Kotov, *Adv. Mater.*, 1999, **11**, 1006.
17 D. S. Koktysh, X. Liang, B. Yun, I. Pastoriza-Santos, R. L. Matts, M. Giersig, C. Serra-Rodriguez, L. M. Liz-Marzan and N. A. Kotov, *Adv. Funct. Mater.*, 2002, **12**, 255.
18 A. Imhof, M. Megens, J. J. Engelberts, D. T. N. de Lang, R. Sprik and W. L. Vos, *J. Phys. Chem. B*, 1999, **103**, 1408.
19 P. Mulvaney, *Langmuir*, 1996, **12**, 788.
20 N. Malikova, I. Pastoriza-Santos, M. Schierhorn, N. A. Kotov and L. M. Liz-Marzan, *Langmuir*, 2002, **18**, 3694.
21 A. Sreekumaran Nair and T. Pradeep, *Chem. Commun.*, submitted for publication in *Angew. Chem., Int. Ed.*
22 D. R. Lide, *CRC Hand Book of Chemistry and Physics*, 80th edn., 1999–2000.
23 G. Mie, *Ann. Physik*, 1908, **25**, 377.
24 S. G. Chaki Sudrik, H. R. Sonawane and K. Vijayamohanan, *Chem. Commun.*, 2002, 76.
25 M. Aslam, N. K. Chaki, I. S. Mulla and K. Vijayamohanan, *Appl. Surf. Sci.*, 2001, **182**, 338.
26 K. Kalyanasundaram and M. Gratzel, in *Optoelectronic Properties of Inorganic Solids*, ed. D. M. Roundhill, J. P. Fackler, Jr., Plenum Press, New York, 1999, p. 169–194.
27 E. F. Lopez, V. S. Escribano, M. Panizza, M. M. Carnasciali and G. Busca, *J. Mater. Chem.*, 2001, **11**, 1891.
28 K. Bandyopadhyay, S. R. Sainkar and K. Vijayamohanan, *J. Am. Ceram. Soc*, 1999, **82**, 222.